

Analytic Few Photon Scattering in Waveguide QED for Entanglement Generation

David L. Hurst* and Pieter Kok†

*Department of Physics and Astronomy, University of Sheffield,
Hounsfield Road, Sheffield, S3 7RH, United Kingdom*

(Dated: July 19, 2017)

We develop an approach to light-matter coupling in waveguide QED based upon scattering amplitudes evaluated via Dyson series. For optical states containing more than single photons, terms in this series become increasingly complex and we provide a diagrammatic recipe for their evaluation, which is capable of yielding analytic results. Our method fully specifies a combined emitter-optical state that permits investigation of matter-matter entanglement generation protocols. We use our expressions to study a scheme for entangling spatially separated two-level systems and find that an entangled two-photon input provides a clear advantage over a separable single photon state.

I. INTRODUCTION

Proposals for devices such as a measurement-based quantum computer [1] or a Quantum Internet [2] require large entangled states with many stationary qubit nodes. Optical photons, with their long coherence times and large velocities, form the ideal carriers of quantum information between these nodes [3] and this means that understanding the light-matter interaction is necessary for the purposes of practical device design. A possible route towards engineering this light-matter interaction involves coupling quantum emitters to the modes of a nanophotonic waveguide. Recently, there has been a great deal of theoretical interest [4, 5] and experimental progress in this field [6–9].

Photon scattering from a two-level system is a relatively well-studied problem, with recent developments including the single and multi-photon scattering matrix [10, 11] and generalisations of the input-output formalism and master equation [12, 13] to waveguide systems. There has also been a substantial body of work focussed on applying techniques from relativistic quantum field theory to the problem, notably the LSZ reduction formula [14], cluster decomposition principle [15] and diagrammatic evaluation of Green's functions [16]. Interest in this simple system remains high today [17, 18], with many authors noting also the possibility of engineering strong on-chip photon-photon interaction [19].

Schemes for engineering entanglement between matter qubits [20, 21] require the stationary qubit state conditional on that of the optical field. We develop a formalism that fully specifies the combined emitter-optical state following photon scattering from a waveguide-embedded emitter. It is interesting to note that despite the apparent simplicity of the two level atom-quantised optical field system, many of the previous approaches involve extremely advanced mathematical techniques and tend not to encourage an intuitive understanding of the global dynamics. This is something that the method we develop

here avoids, with terms in each expression corresponding very naturally to physical processes. We can use this to visualise the processes not allowed by our initial choice of system Hamiltonian.

In this paper, we consider multi-photon scattering from a two-level atom and derive a method to determine the joint state of the atom and photons. In Sec. II we define the waveguide QED system and transition amplitude between arbitrary global system input and output states. In Sec. III, we find an analytic expression for this amplitude when the input optical state consists of a single photon and in Sec IV we develop a diagrammatic recipe for analytically determining the amplitude of a multi-photon process. In Sec. V, we use the single and two-photon transition amplitudes to quantify entanglement generated between spatially separated atoms embedded in a Mach-Zehnder interferometer—such structures are expected to be close to experimental realisation [22]. Sec. VI is reserved for a summary, conclusions and some suggestions for future work.

II. THE SYSTEM

In this section we define quantities associated with the system under consideration, introduce the relevant Hamiltonian and also the transition amplitude between global input and output eigenstates. The two-level system $\{|g\rangle, |e\rangle\}$ has transition frequency Ω with raising and lowering operators σ_+ and σ_- respectively. It is chirally coupled to the right-propagating modes a_ω of an optical waveguide [7–9]. At some time $t_i \rightarrow -\infty$ the system state is given by $|g; \psi_{\text{in}}\rangle$, where ψ_{in} represents the optical wavefunction. A scattering event then occurs, and the global system dynamics are in general complicated to describe until a time $t_f \rightarrow +\infty$, when the emitter has relaxed to its ground level and the optical state $|\psi_{\text{out}}\rangle$ is coupled out of the waveguide. Working in the interaction picture, the input and output states are eigenstates of the free Hamiltonian (H_0) that describes the dynamics of an uncoupled waveguide-emitter system [23]. This allows us to construct input and output states from the usual creation and annihilation operators for photons. The transition amplitude $\mathcal{A} \equiv \langle g; \psi_{\text{out}} | \mathcal{U} | g; \psi_{\text{in}} \rangle$ gives

* dhurst1@sheffield.ac.uk

† p.kok@sheffield.ac.uk

the overlap between an arbitrary output state $|g; \psi_{\text{out}}\rangle$ and an input state evolved from $t \rightarrow -\infty$ to $t \rightarrow +\infty$ by the operator \mathcal{U} . When \mathcal{U} is the time evolution operator evaluated in the interaction picture, the transition amplitude \mathcal{A} completely specifies the global system dynamics. Of course it may be the case that the atom is scattered to some meta-stable or ‘shelved’ state $|s\rangle$. In this case we would instead be evaluating $\langle s; \psi_{\text{out}} | \mathcal{U} | g; \psi_{\text{in}} \rangle$ —which we expect the method presented to readily extend to.

The expansion of \mathcal{U} is known as the Dyson series [24], and takes as an argument the global system interaction Hamiltonian $H_I(t)$. In App. A we show that this is given by ($\hbar = 1$)

$$H_I(t) = \gamma \int d\epsilon (e^{-i\Delta_\epsilon t} \sigma_+ a_\epsilon + e^{i\Delta_\epsilon t} \sigma_- a_\epsilon^\dagger), \quad (1)$$

where the waveguide’s central frequency (around which we linearise the dispersion relation) is denoted by ω_0 , the rate of coupling between photons and the atomic transition is γ^2 and we define $\Delta_\epsilon \equiv \omega_0 + \epsilon - \Omega$. We adopt the convention that unspecified upper and lower integration limits correspond to ∞ and $-\infty$ respectively. We expand the transition amplitude $\mathcal{A} \equiv \mathcal{A}^{(0)} + \mathcal{A}^{(1)} + \mathcal{A}^{(2)} + \dots$ in terms of the Dyson series representation of \mathcal{U} , so that $\mathcal{A}^{(n)} \equiv \langle g; \psi_{\text{out}} | \mathcal{U}^{(n)} | g; \psi_{\text{in}} \rangle$. Using

$$\mathcal{U}^{(n)} = (-i)^n \int dt_1 \int^{t_1} dt_2 \dots \int^{t_{n-1}} dt_n H_I(t_1) H_I(t_2) \dots H_I(t_n), \quad (2)$$

we determine that the n^{th} order term in the transition amplitude contains n copies of the interaction Hamiltonian. For an excitation number conserving Hamiltonian, such as that of Eq. (1), the n^{th} order term corresponds to n absorption/emission processes or $\frac{n}{2}$ combined events. Therefore, the only non-zero contributions to $\mathcal{A}^{(n)}$ are those where n is even and the Pauli matrices are ordered as $\sigma_- \sigma_+ \dots \sigma_- \sigma_+$. The general expression for the n^{th} order term in the transition amplitude is then

$$\mathcal{A}^{(n)} = (-i\gamma)^n \int d\tilde{t}^{(n)} \int d\bar{\epsilon}^{(n)} e^{i(\Delta_{\epsilon_1} t_1 - \Delta_{\epsilon_2} t_2 + \dots - \Delta_{\epsilon_n} t_n)} \times \langle \psi_{\text{out}} | a_{\epsilon_1}^\dagger a_{\epsilon_2} a_{\epsilon_3}^\dagger \dots a_{\epsilon_n} | \psi_{\text{in}} \rangle, \quad (3)$$

where $\int d\tilde{t}^{(n)} \equiv \int dt_1 \int^{t_1} dt_2 \dots \int^{t_{n-1}} dt_n$ and $\int d\bar{\epsilon}^{(n)} \equiv \int d\epsilon_1 \int d\epsilon_2 \dots \int d\epsilon_n$. In the following two sections we show how this quantity, which completely specifies the final system state, can be computed for single and two-photon input states.

III. SINGLE PHOTONS

In this section we demonstrate how to calculate the transition amplitude in Eq. (3) for the situation where a single incident photon with energy $\omega_0 + i$ scatters to an

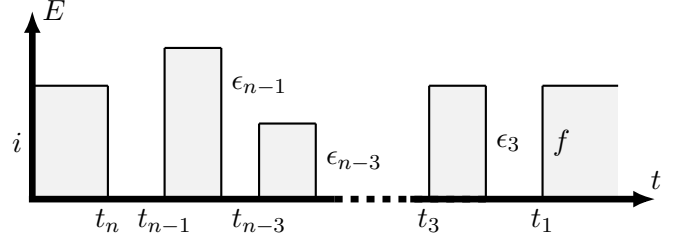


FIG. 1. Diagram for the n^{th} order single photon scattering process. An incident photon of energy $\omega_0 + i$ is scattered to one of frequency $\omega_0 + f$. This occurs via the emission and absorption of $\frac{n}{2} - 1$ ‘internal’ photons.

output photon of energy $\omega_0 + f$. It is simply a matter of applying the bosonic commutation relation to determine $\mathcal{A}^{(0)} = \delta(f - i)$. For $n = 2$ we find

$$\mathcal{A}^{(2)} = -\gamma^2 \int d\tilde{t}^{(2)} \int d\bar{\epsilon}^{(2)} e^{i(\Delta_{\epsilon_1} t_1 - \Delta_{\epsilon_2} t_2)} \times \langle 0 | a_f a_{\epsilon_1}^\dagger a_{\epsilon_2} a_i^\dagger | 0 \rangle, \quad (4)$$

with $|0\rangle$ representing the multi-mode vacuum. We can simplify Eq. (4)

$$\mathcal{A}^{(2)} = -\gamma^2 \int d\tilde{t}^{(2)} e^{i(\Delta_f t_1 - \Delta_i t_2)} = -2\pi\gamma^2 \left[\pi\delta(\Delta_i) + \frac{i}{\Delta_i} \right] \delta(f - i), \quad (5)$$

where the integrals in Eq. (5) were evaluated using the technique found in Ref. [25], reproduced here in App. B. The frequency dependent integration factor will reappear many times, and we define $g(\Delta) \equiv [\pi\delta(\Delta) + i\Delta^{-1}]$ for brevity.

Consider now the n^{th} order term given by

$$\mathcal{A}^{(n)} = (-i\gamma)^n \int d\tilde{t}^{(n)} \int d\bar{\epsilon}^{(n)} e^{i\Delta_{\epsilon_1} t_1 - i\Delta_{\epsilon_2} t_2 \dots - i\Delta_{\epsilon_n} t_n} \langle 0 | a_f a_{\epsilon_1}^\dagger a_{\epsilon_2} \dots a_{\epsilon_n} a_i^\dagger | 0 \rangle, \quad (6)$$

we can use the vacuum expectation value in (6) to eliminate the first, final and half of the remaining frequency integrals

$$\mathcal{A}^{(n)} = (-i\gamma)^n \int d\tilde{t}^{(n)} \int d\epsilon_3 d\epsilon_5 \dots d\epsilon_{n-1} e^{i(\Delta_f t_1 - \Delta_{\epsilon_3} t_2 + \Delta_{\epsilon_5} t_3 + \dots \Delta_i t_n)}. \quad (7)$$

It is quite easy to understand the nature of the physical process described by Eq. (7) and we have sketched it explicitly in Fig. 1. We see that the atom absorbs the original incident photon and, before emitting the outgoing photon, emits and absorbs $\frac{n}{2} - 1$ photons of frequencies $\{\epsilon_{n-1}, \epsilon_{n-3} \dots \epsilon_3\}$. The energies of these ‘internal’ photons are uncertain and we integrate over a continuum of

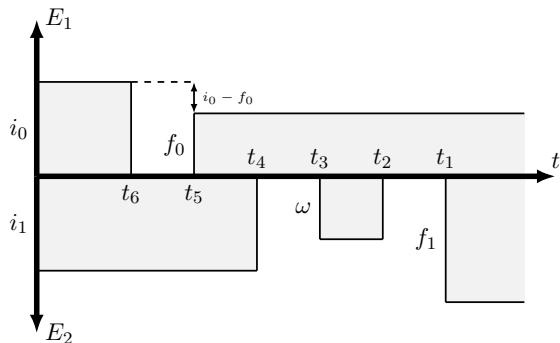


FIG. 2. Diagram for one of the possible $n = 6$ processes. Incident photons of energy $\omega_0 + i_{0/1}$ are scattered to energies $\omega_0 + f_{0/1}$. An internal photon ‘loop’ of energy ω occurs, and ω is integrated over.

possible values for each, which has the effect of reducing their duration to zero—a ‘point-like’ interaction.

The integrand in (7) can be further decomposed into its constituent Dirac delta functions and we have then

$$\mathcal{A}^{(n)} = (-i\gamma)^n (2\pi)^{\left(\frac{n}{2}-1\right)} \int dt_1 e^{i\Delta_f t_1} \int^{t_1} dt_2 \int^{t_2} dt_3 \delta(t_3 - t_2) \dots \int^{t_{n-1}} dt_n e^{-i\Delta_i t_n}. \quad (8)$$

Successively performing time integrals in exactly the same manner as for the second order case, we arrive upon

$$\mathcal{A}^{(n)} = 2(-i\gamma)^n \delta(f - i) (\pi g(\Delta_i))^{\frac{n}{2}}. \quad (9)$$

Summing over even n and using the binomial theorem, we find

$$\mathcal{A} = \frac{1 - \gamma^2 \pi g(\Delta_i)}{1 + \gamma^2 \pi g(\Delta_i)} \delta(f - i) \equiv t(i) \delta(f - i), \quad (10)$$

which is valid under the condition $|\pi\gamma^2 g(\Delta_i)| < 1$ —corresponding to the case where the rate of coupling between the emitter and photon is strictly smaller than their detuning. Eq. (10) is the first key result of this work and demonstrates that our method yields non-perturbative expressions for the single-photon transition amplitude. In App. E we demonstrate its equivalence to the result of Fan *et al* [10].

IV. DIAGRAMMATIC APPROACH

In this section we elaborate further on the diagrammatic method alluded to in Sec. III in order to evaluate the two-photon transition amplitude. For photons with energies $\omega_0 + i_0$ and $\omega_0 + i_1$, the n^{th} order transition amplitude is

$$\mathcal{A}^{(n)} = (-i\gamma)^n \int d\vec{t}^{(n)} \int d\vec{\epsilon}^{(n)} e^{i(\Delta_{\epsilon_1} t_1 - \Delta_{\epsilon_2} t_2 \dots - \Delta_{\epsilon_n} t_n)} \times \langle 0 | a_{f_0} a_{f_1} a_{\epsilon_1}^\dagger a_{\epsilon_2} \dots a_{\epsilon_n} a_{i_1}^\dagger a_{i_0}^\dagger | 0 \rangle, \quad (11)$$

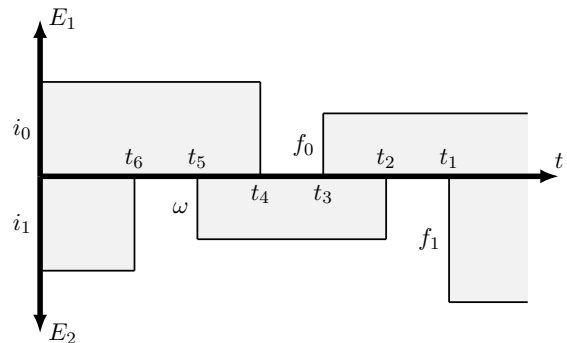


FIG. 3. Diagram for one of the impossible $n = 6$ processes. Incident photons of energy $\omega_0 + i_{0/1}$ are scattered to energies $\omega_0 + f_{0/1}$. An internal photon ‘loop’ of energy ω occurs, and ω is integrated over.

where f_0 and f_1 label the scattered photon frequencies. Evaluation of the vacuum expectation value in the integrand of Eq. (11) produces $2^{\frac{n}{2}+1}$ terms and it is not feasible to mechanically calculate these. We instead use the physical interpretation of each term to provide further guidance.

For example, consider one of the sixteen terms contributing to $\mathcal{A}^{(6)}$

$$\mathcal{A}_{(1)}^{(6)} = -\gamma^6 \int d\vec{t}^{(6)} \int d\omega e^{i(\Delta_{f_1} t_1 - \Delta_\omega (t_2 - t_3) - \Delta_{i_1} t_4 + \Delta_{f_0} t_5 - \Delta_{i_0} t_6)}, \quad (12)$$

which, using exactly the same integration techniques as for the single-photon case, reduces to

$$\mathcal{A}_{(1)}^{(6)} = -2\pi^2 \gamma^6 \delta(f_0 + f_1 - i_0 - i_1) g(\Delta_{i_0}) g(\Delta_{i_0} - \Delta_{f_0}) g(\Delta_{i_0} + \Delta_{i_1} - \Delta_{f_0})^2. \quad (13)$$

By re-associating bosonic mode operators to their phases in the integrand of Eq. (12) we deduce that this term describes absorption by the atom of a photon with energy $\omega_0 + i_0$, prior to emission of a final $\omega_0 + f_0$ photon. Subsequently, the second incident photon is absorbed and emitted twice via an intermediate step of energy $\omega_0 + \omega$. Fig. 2 gives a pictorial representation of the process, with time evolving from left-to-right and energies of the two populated modes relative to ω_0 given by the distance from the horizontal axis.

We can derive amplitudes in general from diagrams such as Fig. 2. By drawing the diagrams corresponding to the possible emission/absorption processes we can calculate the total transition amplitude. With each emission and absorption event in a diagram we associate a number Δ representing the difference between the total amount of absorbed radiation by the atom and the ground-excited energy gap. In Fig. 2, the atom absorbs a photon of frequency $\omega_0 + i_0$ (yielding Δ_{i_0}), and emits a photon with energy $\omega_0 + f_0$ yielding $\Delta_{i_0} - \Delta_{f_0}$ corresponding to the residual energy between the two photons.

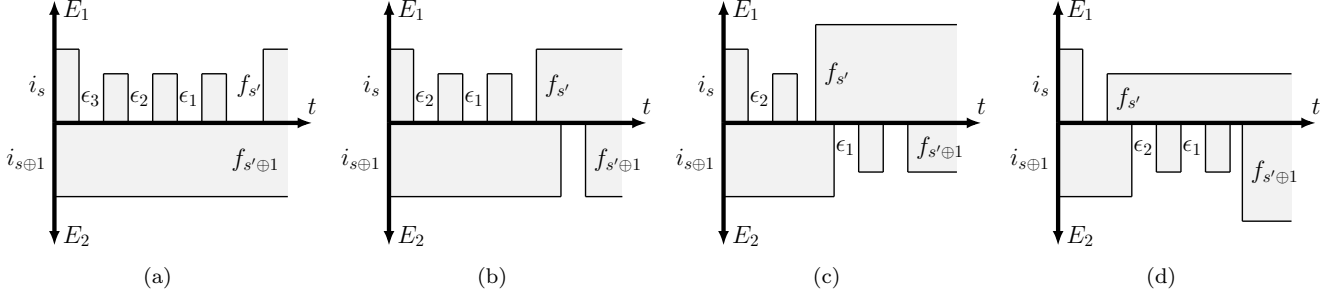


FIG. 4. The four non-zero types of diagram for the $\mathcal{A}^{(8)}$ term in the expansion of the two photon amplitude. Fig. 4a represents the non-frequency mixing term.

Absorbing the second incident photon produces the factor $\Delta_{i_0} + \Delta_{i_1} - \Delta_{f_0}$. These terms appear as arguments of the frequency dependent function $g(x)$ in Eq. (13), which describes the amplitude of the process depicted in Fig. 2. The ‘loop’ indicated by ω in Fig. 2 increases the power of $g(\Delta_{i_0} + \Delta_{i_1} - \Delta_{f_0})$ by one. Finally, we impose energy conservation via $\delta(f_0 + f_1 - i_0 - i_1)$.

Suppose that for a given n we have drawn all diagrams corresponding to $\frac{n}{2}$ light-matter interaction events. Four of these diagrams (the permutations over initial and final photon frequencies) will always have one photon interacting with the emitter $\frac{n}{2}$ times, with the second photon passing through unperturbed (i.e., non-frequency mixing terms). These diagrams contribute amplitudes equivalent to the single photon case. Another class of diagrams we immediately discard is that in which an ‘internal’ photon (such as ω in Fig. 2) is emitted at time t_m and *not* reabsorbed at $t = t_{m-1}$, since the interval $[t_m, t_{m-1}] \rightarrow 0$. We rigorously demonstrate this in App. C. The remaining diagrams are similar in structure to Fig. 2, with initial absorption and final emission separated by a number of internal photon loops. The structure of the integrals corresponding to these diagrams is the same as in Eq. (12) with additional frequency and time integrals corresponding to these internal loops.

The procedure for converting diagrams into $\mathcal{A}^{(n)}$ is as follows:

- (i) draw all possible diagrams with $\frac{n}{2}$ total interactions;
- (ii) identify the single photon (non-frequency mixing) terms;
- (iii) discard the terms in which internal photons are emitted and not immediately reabsorbed;
- (iv) the remaining terms get the constant pre-factor $\frac{2}{\pi}(i\sqrt{\pi}\gamma)^n$;
- (v) each absorption event gets a factor $g(\Delta)$, where Δ corresponds to the total absorbed radiation, and each emission event gets $g(\Delta_{\text{res}})$, where Δ_{res} is the amount of absorbed radiation not re-emitted;
- (vi) for each loop, multiply by an additional factor of

$g(\Delta)$ with the same Δ as at the previous absorption;

- (vii) at the final emission, multiply by $\delta(f_0 + f_1 - i_0 - i_1)$.

The four species of diagram for the $n = 8$ case are shown in Fig. 4 and in App. D we explicitly perform this procedure to demonstrate equivalence between the diagrammatic and integral methods.

One interesting observation here is that for $n \geq 6$ the particular form of Eq. (1) causes vanishing of the terms with internal photon emission not immediately followed by re-absorption (step (iii) of the above outlined rules). This behaviour is due to the Hamiltonian’s instantaneous coupling between the emitter and continuum of waveguide modes (without cut-off) at a constant rate. It is interesting to note that this oft-employed model makes this prediction and still agrees well with experimental data. General Hamiltonians with discretised waveguide modes would not necessarily lead to these terms vanishing. We show one of these dis-allowed diagrams in Fig. 3.

Let the frequency mixing term in $\mathcal{A}^{(n)}$ for the two-photon case be given by $\delta(f_0 + f_1 - i_0 - i_1)\mathcal{M}^{(n)}$. From the above procedure we deduce that the total photon frequency mixing term in the two-photon transition amplitude is given by $\mathcal{M} = \sum_{n=2}^{\infty} \mathcal{M}^{(n)}$ where:

$$\mathcal{M}^{(n)} = \sum_{s=0,1} \sum_{s'=0,1} g(\Delta_{i_s})g(\Delta_{i_s} - \Delta_{f_{s'}})g(\Delta_{f_{s'⊕1}}) \frac{2}{\pi}(-\pi\gamma^2)^n \sum_{k=0}^{n-2} g(\Delta_{i_s})^k g(\Delta_{f_{s'⊕1}})^{n-2-k} \quad (14)$$

The sum over k can be evaluated [26], and we sum over all n to find \mathcal{M} . Adding this to the non-frequency mixing component yields a final expression for the two-photon

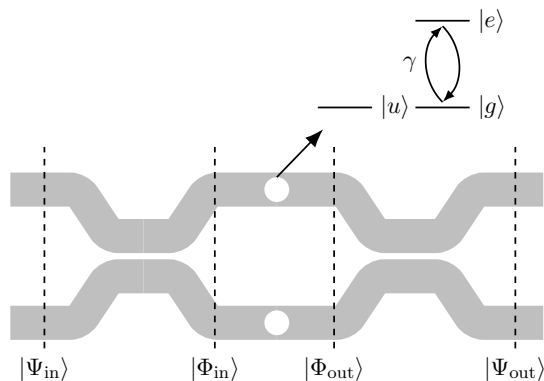


FIG. 5. Mach-Zehnder interferometer where the optical modes in each arm are coupled at a rate γ to the $|g\rangle \rightarrow |e\rangle$ transition of an emitter with L -type energy level configuration.

transition amplitude:

$$\begin{aligned} \mathcal{A} = & [t(i_0) + t(i_1) - 1] \\ & \times [\delta(f_0 - i_0)\delta(f_1 - i_1) + \delta(f_0 - i_1)\delta(f_1 - i_0)] \\ & + 2\pi\gamma^4\delta(f_0 + f_1 - i_0 - i_1) \sum_{s=0,1} \sum_{s'=0,1} \\ & \frac{g(\Delta_{i_s})g(\Delta_{i_s} - \Delta_{f_{s'}\oplus 1})g(\Delta_{f_{s'}\oplus 1})}{[1 + \pi\gamma^2g(\Delta_{i_s})][1 + \pi\gamma^2g(\Delta_{f_{s'}\oplus 1})]}, \end{aligned} \quad (15)$$

where $t(i)$ is defined in Eq. (10) and we have assumed that γ^2 remains smaller than the initial and final photon-atom detunings. Eq. (15) is the second main result of this work and demonstrates our formalism's power to produce non-perturbative amplitudes for multi-photon processes. We demonstrate its equivalence to the expression found by Fan *et al* in App. E.

V. ENTANGLEMENT GENERATION

As an application, we describe a protocol for simple generation of entanglement between stationary qubits. In contrast to many previously reported protocols, this method does not rely on strong-coupling between the waveguide and emitter and is able to generate small quantities of entanglement for modest coupling strengths. This could in future be paired with distillation procedures to generate maximally entangled qubit pairs. Consider two emitters, with L -type level structure, chirally coupled to upper and lower waveguides in a Mach-Zehnder interferometer, shown in Fig. 5. The qubit states are $|u\rangle$ and $|g\rangle$, and $|u\rangle$ is uncoupled from $|g\rangle$ and $|e\rangle$ while the $|g\rangle \rightarrow |e\rangle$ transition is optically allowed. We have control over the optical states into the upper (a) and lower (b) interferometer arms and monitor both output ports.

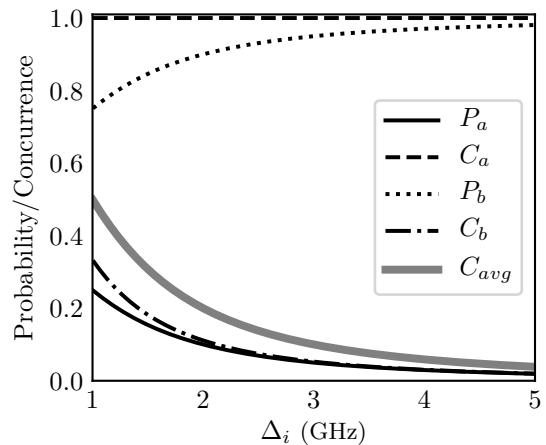


FIG. 6. Probability of photon detection and subsequent atomic concurrence for output ports a and b with $\gamma = \pi^{-\frac{1}{2}} \text{GHz}^{\frac{1}{2}}$ as a function of emitter-photon detuning. $P_{a/b}$ describe the probabilities of photo-detection at the two output ports and $C_{a/b}$ the concurrence of the subsequent atomic state. C_{avg} gives the resulting average concurrence as the number of experiments becomes large.

There are many possible routes to entanglement generation in systems such as this (e.g., [21]). First, consider injection of a single photon (with frequency $\omega_0 + i$) into input a . Time evolution of the system is divided into four discrete phases: $|\Psi_{in}\rangle \rightarrow |\Phi_{in}\rangle \rightarrow |\Phi_{out}\rangle \rightarrow |\Psi_{out}\rangle$. The system states at the beginning and end of the procedure are denoted by $|\Psi_{in}\rangle$ and $|\Psi_{out}\rangle$ respectively. The intermediate states $|\Phi_{in}\rangle$ and $|\Phi_{out}\rangle$ describe the system immediately before and after the light-matter interaction.

For a single photon procedure, $|\psi_{in}^a\rangle = |i\rangle$ and $|\psi_{in}^b\rangle = |0\rangle$. With both emitters prepared initially in the state $\frac{1}{\sqrt{2}}(|u\rangle + |g\rangle)$, the state $|\Psi_{out}\rangle$ depends on the phase accumulated by the $|g\rangle$ component of the initial atomic state, which can in turn be found from the transition amplitude (10). After performing this calculation (outlined explicitly in App. F), we find the reduced density matrix describing the atomic system conditioned on the detection of a photon at output a or b . From this, we determine the concurrence [27], along with the probability of photon detection at each output, shown in Fig. 6.

An important question is how the optical input state affects the amount of entanglement between the stationary matter qubits. For example, sending two identical photons into the beam-splitter arms ($|\psi_{in}^a, \psi_{in}^b\rangle = |\omega_0 + i, \omega_0 + i\rangle$) leads to a two-photon NOON state impinging the atoms via the Hong-Ou-Mandel effect [28]. In this case there are six possible measurement outcomes: detecting two photons at either output port or one at each and finding the detected photons to be frequency mixed or not. Their probabilities and associated atomic states depend on the light-matter coupling strength. Fig. 7 shows the weighted average concurrence

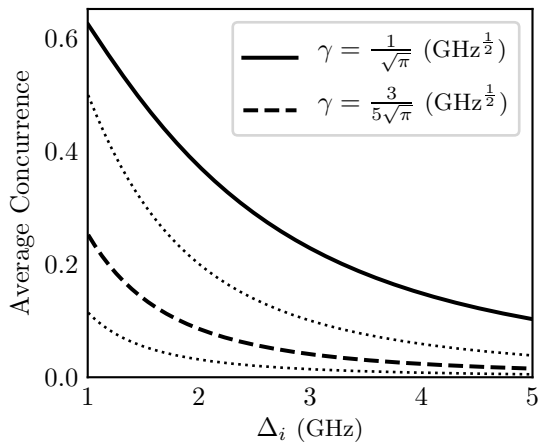


FIG. 7. Average concurrence over all possible detection events for two coupling strengths. Dotted lines below the solid and dashed lines represent the equivalent average concurrences for the single-photon input states.

over all possible detection events for one and two photon input states. A sizeable enhancement is possible using multiple input photons, surprisingly (for larger detunings) exceeding the factor 2 that might naively have been expected from the two-photon NOON state.

VI. CONCLUSIONS

We have developed an intuitive, diagrammatic approach to the problem of light-matter coupling in waveguide QED. In contrast to previously reported techniques, our method allows visualisation of the photon-atom dynamics, along with analysis of schemes for generating entanglement between stationary matter qubits. We have demonstrated analytical results for both single and two photon input optical states and have been able to exactly quantify the increase in entanglement generated when using a two-photon input. The diagrammatic approach is straight-forward to extend to higher photon number input states and more realistic Hamiltonians, and analytic results are expected to follow. Several open questions emerge from this work. For instance, how does the choice of Hamiltonian in Eq. (1) impact the transition amplitude? In particular, a waveguide will have a range of supported frequency modes defined largely by its dimensions. Does this lead to previously unreported observable consequences—a modification to the amplitude due to the inclusion of additional diagrams? The limit on our method is ultimately a computational one, with an N -photon event requiring N permutations over both initial and final frequencies.

DLH acknowledges useful suggestions from M.E. Pearce and is supported by an EPSRC studentship.

Appendix A: The Hamiltonian

In this appendix we derive the interaction Hamiltonian (1) that describes the waveguide QED system. We begin by dividing the total Hamiltonian into free and interacting parts, H_0 and H_{int} respectively. The dynamics of an isolated emitter and bare waveguide are described by H_0 , while the coupling between them—which we assume is of dipole form—is specified by H_{int} . We take a limit where the waveguide supports a continuum of optical modes with wavenumber k and also make the rotating-wave approximation. This leads to

$$H_0 = \frac{1}{2}\Omega\sigma_z + \int_0 dk \omega(k)\tilde{a}_k^\dagger\tilde{a}_k$$

$$H_{\text{int}} = \tilde{\gamma} \int_0 dk \left(\sigma_+\tilde{a}_k + \tilde{a}_k^\dagger\sigma_- \right), \quad (\text{A1})$$

where $\omega(k)$ gives the waveguide dispersion relation and the operator \tilde{a}_k destroys a photon of wavenumber k while obeying $[\tilde{a}_k, \tilde{a}_{k'}^\dagger] = \delta(k - k')$. We have assumed the fixed coupling rate $\tilde{\gamma}$ between optical modes of wavenumber k and atomic transition and adopted the convention that unspecified lower and upper integration limits imply negative and positive infinity respectively.

It is shown by e.g. Maier [29] that the dispersion relation for waveguide confined optical modes is surface-plasmonic. We linearise this about some central wavenumber k_0 so that: $\tilde{\omega}(k) \approx \omega_0 + v_g(k - k_0)$, where v_g represents the photon group velocity. This means that

$$H_0 = \frac{1}{2}\Omega\sigma_z + \int dk \omega_0\tilde{a}_k^\dagger\tilde{a}_k + v_g(k - k_0)\tilde{a}_k^\dagger\tilde{a}_k$$

$$H_{\text{int}} = \tilde{\gamma} \int dk \left(\sigma_+\tilde{a}_k + \tilde{a}_k^\dagger\sigma_- \right), \quad (\text{A2})$$

where we have also extended the limits of integration to cover the entirety of wavenumber space—an appropriate approximation when the band of populated modes is narrow. We next introduce the variable: $\epsilon \equiv v_g(k - k_0)$, which we use to re-write the Hamiltonian

$$H_0 = \frac{1}{2}\Omega\sigma_z + \int d\epsilon (\omega_0 + \epsilon)a_\epsilon^\dagger a_\epsilon$$

$$H_{\text{int}} = \gamma \int d\epsilon (\sigma_+ a_\epsilon + \sigma_- a_\epsilon^\dagger) \quad (\text{A3})$$

where we have defined $\gamma \equiv v_g^{-\frac{1}{2}}\tilde{\gamma}$ and $a_\epsilon = v_g^{-\frac{1}{2}}\tilde{a}_{k_0+v_g^{-1}\epsilon}$. It can be easily shown that the commutation relation $[a_\epsilon, a_{\epsilon'}^\dagger] = \delta(\epsilon - \epsilon')$ is preserved.

At this point we can simply use the definition of the interaction Hamiltonian [23] and equation (A3) to deduce that

$$H_I(t) = \gamma \int d\epsilon (e^{-i\Delta_\epsilon t}\sigma_+ a_\epsilon + e^{i\Delta_\epsilon t}\sigma_- a_\epsilon^\dagger), \quad (\text{A4})$$

which is the desired result with the detuning defined by $\Delta_\epsilon \equiv \omega_0 + \epsilon - \Omega$. The last point to note is the slight difference in structure between Hamiltonian (A4) and the

version used by other authors (e.g. [10]). The discrepancies can be ascribed simply to our not working in a frame rotating at the waveguide's central frequency and our inclusion of the free emitter Hamiltonian in H_0 as opposed to H_{int} .

Appendix B: Integration Technique

For completeness we describe here the integration technique used to evaluate the explicit integral expressions for the single and two photon transition amplitudes. This is a relatively well-known result and can be found in e.g. the appendix of [25]. We define the integral \mathcal{I} and begin by changing variables so as to shift the limits of integration

$$\mathcal{I} \equiv \int_{-\infty}^{t_1} dt_2 e^{-i\Delta_i t_2} = \int_0^{\infty} dt_2 e^{-i\Delta_i(t_1-t_2)}.$$

This can be decomposed and multiplied by unity to give

$$\mathcal{I} = e^{-i\Delta_i t_1} \lim_{\alpha \rightarrow 0} \int_0^{\infty} dt_2 e^{-\alpha t_2} [\cos(\Delta_i t_2) + i \sin(\Delta_i t_2)] \quad (\text{B1})$$

and we then make use of standard results [30], for example noting

$$\delta(x) = \frac{1}{\pi} \lim_{\alpha \rightarrow 0} \frac{\alpha}{\alpha^2 + x^2} \quad (\text{B2})$$

to find that

$$\begin{aligned} \mathcal{I} &= e^{-i\Delta_i t_1} \lim_{\alpha \rightarrow 0} \left(\frac{\alpha}{\alpha^2 + \Delta_i^2} + i \frac{\Delta_i}{\alpha^2 + \Delta_i^2} \right) \\ &= e^{-i\Delta_i t_1} \left(\pi \delta(\Delta_i) + \frac{i}{\Delta_i} \right), \end{aligned} \quad (\text{B3})$$

which is the desired formula.

Appendix C: Vanishing Terms in Higher Order Transition Amplitudes

In this appendix we show mathematically why diagrams with internal photon loops spanning multiple time integrals, as described in Sec. IV and shown in Fig. 3, should be discarded. If we methodically calculate $\mathcal{A}^{(6)}$ we arrive

upon many terms, for example

$$-\gamma^6 \int d\tilde{t}^{(6)} \int d\omega e^{i(\Delta_{f_1} t_1 - \Delta_{\omega}(t_2 - t_5) + \Delta_{f_0} t_3 - \Delta_{i_0} t_4 - \Delta_{i_1} t_6)}. \quad (\text{C1})$$

Evaluation of the frequency integral in this expression yields the Dirac delta function $\delta(t_5 - t_2)$ and so we are evaluating an integral of the form

$$\int^{t_2} dt_3 \int^{t_3} dt_4 \int^{t_4} dt_5 h(t_5, t_4, t_3) \delta(t_5 - t_2), \quad (\text{C2})$$

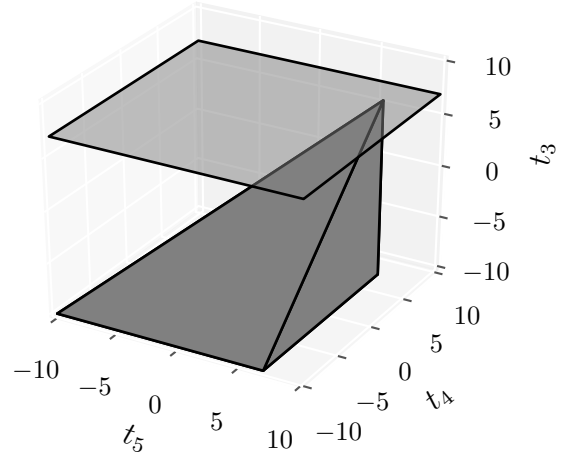


FIG. 8. Integration region defined by the enclosed volume. We see that it intersects the surface defined by $t_5 = t_2$ at only a single point.

where $h(t_5, t_4, t_3)$ is some exponential function. The integral here is over a volume in time-space, bounded by the surfaces $t_5 = t_4$ and $t_4 = t_3$. The delta function has the effect of converting this volume integral into one over a surface—where the surface is defined by projection of the original volume onto $t_5 = t_2$. A representation of this is depicted in Figure 8 and we see that the resulting surface is given by a point. This term therefore does not contribute to the transition amplitude.

Appendix D: Integral and Diagrammatic Evaluation of $\mathcal{A}^{(8)}$ for the Two Photon Case

1. Direct Integration Approach

In this appendix we demonstrate that for $n = 8$ the diagrammatic and integral approaches to evaluation of the n^{th} order transition amplitude agree. By definition we have that

$$\mathcal{A}^{(8)} = \gamma^8 \int d\tilde{t}^{(8)} \int d\tilde{\epsilon}^{(8)} e^{i(\Delta_{\epsilon_1} t_1 - \Delta_{\epsilon_2} t_2 + \Delta_{\epsilon_3} t_3 - \Delta_{\epsilon_4} t_4 + \Delta_{\epsilon_5} t_5 - \Delta_{\epsilon_6} t_6 + \Delta_{\epsilon_7} t_7 - \Delta_{\epsilon_8} t_8)} \times \langle 0 | a_{f_0} a_{f_1} a_{\epsilon_1}^\dagger a_{\epsilon_2} a_{\epsilon_3}^\dagger a_{\epsilon_4} a_{\epsilon_5}^\dagger a_{\epsilon_6} a_{\epsilon_7}^\dagger a_{\epsilon_8} a_{i_1}^\dagger a_{i_0}^\dagger | 0 \rangle. \quad (\text{D1})$$

The vacuum-expectation-value in this expression can be directly evaluated and we find expressions for a total of thirty-two terms

$$\begin{aligned} \mathcal{A}^{(8)} = \gamma^8 \int d\tilde{t}^{(8)} \int d\epsilon_1 \int d\epsilon_2 & \left[e^{i(\Delta_{f_0} t_1 - \Delta_{\epsilon_1} t_2 + \Delta_{f_1} t_3 - \Delta_{\epsilon_2} t_4 + \Delta_{\epsilon_1} t_5 - \Delta_{i_1} t_6 + \Delta_{\epsilon_2} t_7 - \Delta_{i_0} t_8)} \right. \\ & + e^{i(\Delta_{f_1} t_1 - \Delta_{\epsilon_1} t_2 + \Delta_{f_0} t_3 - \Delta_{\epsilon_2} t_4 + \Delta_{\epsilon_1} t_5 - \Delta_{i_1} t_6 + \Delta_{\epsilon_2} t_7 - \Delta_{i_0} t_8)} \\ & + \dots \\ & \left. + e^{i(\Delta_{f_1} t_1 - \Delta_{i_0} t_2 + \Delta_{f_0} t_3 - \Delta_{\epsilon_2} t_4 + \Delta_{\epsilon_2} t_5 - \Delta_{\epsilon_1} t_6 + \Delta_{\epsilon_1} t_7 - \Delta_{i_1} t_8)} \right] \end{aligned} \quad (\text{D2})$$

where we have used the delta functions from the decomposed vacuum-expectation-value to eliminate six of the eight frequency integrals. We can then use the definition of the Dirac delta function to transform the remaining frequency integrals and integrands into delta functions in time. Using the method outlined in App. C, we can then eliminate any term with a delta function connecting non-adjacent times (e.g. $\delta(t_7 - t_4)$, $\delta(t_4 - t_1)$ etc.) and sixteen terms remain. There are however only four ‘categories’ of term—with each category containing four terms that are permutations over initial and final photon energies. We find that

$$\begin{aligned} \mathcal{A}^{(8)} = (2\pi)^2 \gamma^8 \sum_{s=0,1} \sum_{s'=0,1} \int d\tilde{t}^{(8)} & \left[2\pi \delta(f_{s'} - i_s) \right. \\ & \delta(t_7 - t_6) \delta(t_5 - t_4) \delta(t_3 - t_2) e^{i(\Delta_{f_{s' \oplus 1}} t_1 - \Delta_{i_{s \oplus 1}} t_8)} \\ & + \delta(t_7 - t_6) \delta(t_5 - t_4) e^{i(\Delta_{f_{s'}} t_1 - \Delta_{i_{s \oplus 1}} t_2 + \Delta_{f_{s' \oplus 1}} t_3 - \Delta_{i_s} t_8)} \\ & + \delta(t_3 - t_2) \delta(t_7 - t_6) e^{i(\Delta_{f_{s'}} t_1 - \Delta_{i_{s \oplus 1}} t_4 + \Delta_{f_{s' \oplus 1}} t_5 - \Delta_{i_s} t_8)} \\ & \left. + \delta(t_5 - t_4) \delta(t_3 - t_2) e^{i(\Delta_{f_{s'}} t_1 - \Delta_{i_{s \oplus 1}} t_6 + \Delta_{f_{s' \oplus 1}} t_7 - \Delta_{i_s} t_8)} \right]. \end{aligned} \quad (\text{D3})$$

The integrals in Eq. (D3) can be evaluated directly, as in the main text for $n = 6$ and we find

$$\begin{aligned} \mathcal{A}^{(8)} = 2\pi^3 \gamma^8 \sum_{s=0,1} \sum_{s'=0,1} & \left[\pi g^4(\Delta_{i_s}) \delta(f_{s'} - i_s) \delta(f_{s' \oplus 1} - i_{s \oplus 1}) \right. \\ & + g^3(\Delta_{i_s}) g(\Delta_{i_s} - \Delta_{f_{s'}}) g(\Delta_{f_{s' \oplus 1}}) \delta(f_0 + f_1 - i_0 - i_1) \\ & + g^2(\Delta_{i_s}) g(\Delta_{i_s} - \Delta_{f_{s'}}) g^2(\Delta_{f_{s' \oplus 1}}) \delta(f_0 + f_1 - i_0 - i_1) \\ & \left. + g(\Delta_{i_s}) g(\Delta_{i_s} - \Delta_{f_{s'}}) g^3(\Delta_{f_{s' \oplus 1}}) \delta(f_0 + f_1 - i_0 - i_1) \right], \end{aligned} \quad (\text{D4})$$

which is the final result for the $n = 8$ term in the two-photon transition amplitude.

2. Diagrammatic Method

The diagrams corresponding to the four species of term in Eqn. (D3) are shown in Fig. 4. In Fig. 4a a single photon is absorbed and emitted by the atom four times, in Fig. 4b a photon is absorbed and emitted three times, before a second photon is absorbed and emitted once. Fig. 4c shows both photons being absorbed and emitted twice and the Fig. 4d shows a single absorption/emission for the first photon, followed by three for the second. Diagram 4a represents the non-frequency mixing component of the $n = 8$ term and therefore contributes a factor of $2\pi^4 \gamma^8 g^4(\Delta_{i_s}) \delta(f_{s'} - i_s) \delta(f_{s' \oplus 1} - i_{s \oplus 1})$ to the amplitude—this being the single photon result multiplied by an additional delta function to impose conservation of energy for the second photon.

The three frequency mixing diagrams require application of the rules supplied in the main text. For example, consider the diagram shown in Fig. 4c. We first associate the pre-factor $2\pi^3 \gamma^8$ to this diagram’s term, substituting $n = 8$ into the expression $\frac{2}{\pi} (\sqrt{\pi} \gamma)^n$ for the n^{th} order case. The first absorption event then yields a factor of $g(\Delta_{i_s})$ as per the rules and we gain an additional factor of this term from the internal emission and absorption of the ϵ_1 photon. Emission of the photon with frequency $f_{s'}$ then yields the factor $g(\Delta_{i_s} - \Delta_{f_{s'}})$ before the next incident photon is absorbed, producing $g(\Delta_{i_{s \oplus 1}} + \Delta_{i_s} - \Delta_{f_{s'}})$. One additional copy of this factor is required, because of the second internal photon emission/absorption process but its argument can be simplified, as the final emission event yields the factor $\delta(f_0 + f_1 - i_0 - i_1)$, meaning that $\Delta_{i_{s \oplus 1}} + \Delta_{i_s} - \Delta_{f_{s'}} = \Delta_{f_{s' \oplus 1}}$. Multiplying individual factors together yields the expression $2\pi^3 \gamma^8 g^2(\Delta_{i_s}) g(\Delta_{i_s} - \Delta_{f_{s'}}) g^2(\Delta_{f_{s' \oplus 1}}) \delta(f_0 + f_1 - i_0 - i_1)$, exactly as found in Eq. (D4).

Appendix E: Equivalence to Fan Result

In this section we demonstrate equivalence between our results for the single and two-photon transition amplitudes and expressions for the scattering matrix found by Fan *et al.* [10]. As our transition amplitudes are evaluated in the limit $t \rightarrow \infty$ the scattering matrix is in fact the quantity given by these amplitudes. For the single photon case we find that

$$\mathcal{A} = \frac{1 - \pi\gamma^2 g(\Delta_i)}{1 + \pi\gamma^2 g(\Delta_i)} \delta(f - i). \quad (\text{E1})$$

We can substitute our definition of $g(\Delta)$ into Eq. (E1) to determine

$$\mathcal{A} = \frac{\Delta_i - i\pi\gamma^2 - \pi^2\gamma^2 \Delta_i \delta(\Delta_i)}{\Delta_i + i\pi\gamma^2 + \pi^2\gamma^2 \Delta_i \delta(\Delta_i)} \delta(f - i) \quad (\text{E2})$$

which is naturally equal to that found by Fan *et al.*

$$\mathcal{A} = \frac{\Delta_i - i\pi\gamma^2}{\Delta_i + i\pi\gamma^2} \delta(f - i). \quad (\text{E3})$$

The two-photon result requires a little more effort, our result is that

$$\begin{aligned} \mathcal{A} = & [t(i_0) + t(i_1) - 1] \\ & \times [\delta(f_0 - i_0)\delta(f_1 - i_1) + \delta(f_0 - i_1)\delta(f_1 - i_0)] \\ & + 2\pi\gamma^4 \delta(f_0 + f_1 - i_0 - i_1) \sum_{s=0,1} \sum_{s'=0,1} \\ & \frac{g(\Delta_{i_s})g(\Delta_{i_s} - \Delta_{f_{s'}})g(\Delta_{f_{s' \oplus 1}})}{[1 + \pi\gamma^2 g(\Delta_{i_s})][1 + \pi\gamma^2 g(\Delta_{f_{s' \oplus 1}})]}. \end{aligned} \quad (\text{E4})$$

Now, if we expand out the factor $g(\Delta_{i_s} - \Delta_{f_{s'}})$ so that

$$\begin{aligned} & \frac{g(\Delta_{i_s})g(\Delta_{i_s} - \Delta_{f_{s'}})g(\Delta_{f_{s' \oplus 1}})}{[1 + \pi\gamma^2 g(\Delta_{i_s})][1 + \pi\gamma^2 g(\Delta_{f_{s' \oplus 1}})]} = \\ & \frac{\pi g(\Delta_{i_s})\delta(\Delta_{i_s} - \Delta_{f_{s'}})g(\Delta_{f_{s' \oplus 1}})}{[1 + \pi\gamma^2 g(\Delta_{i_s})][1 + \pi\gamma^2 g(\Delta_{f_{s' \oplus 1}})]} \\ & + \frac{ig(\Delta_{i_s})g(\Delta_{f_{s' \oplus 1}})}{(\Delta_{i_s} - \Delta_{f_{s'}})[1 + \pi\gamma^2 g(\Delta_{i_s})][1 + \pi\gamma^2 g(\Delta_{f_{s' \oplus 1}})]}. \end{aligned} \quad (\text{E5})$$

It is then true that

$$\begin{aligned} \mathcal{A} = & [t(i_0) + t(i_1) - 1][\delta(f_0 - i_0)\delta(f_1 - i_1) + \delta(f_0 - i_1)\delta(f_1 - i_0)] \\ & + 4\pi^2\gamma^4 [\delta(f_0 - i_0)\delta(f_1 - i_1) + \delta(f_0 - i_1)\delta(f_1 - i_0)] \frac{g(\Delta_{i_0})g(\Delta_{i_1})}{[1 + \pi\gamma^2 g(\Delta_{i_0})][1 + \pi\gamma^2 g(\Delta_{i_1})]} \\ & + 2\pi i\gamma^4 \delta(f_0 + f_1 - i_0 - i_1) \left[\frac{g(\Delta_{i_0})g(\Delta_{f_0})}{(\Delta_{i_0} - \Delta_{f_1})[1 + \pi\gamma^2 g(\Delta_{i_0})][1 + \pi\gamma^2 g(\Delta_{f_0})]} \right. \\ & + \frac{g(\Delta_{i_0})g(\Delta_{f_1})}{(\Delta_{i_0} - \Delta_{f_0})[1 + \pi\gamma^2 g(\Delta_{i_0})][1 + \pi\gamma^2 g(\Delta_{f_1})]} + \frac{g(\Delta_{i_0})g(\Delta_{f_1})}{(\Delta_{i_1} - \Delta_{f_0})[1 + \pi\gamma^2 g(\Delta_{i_1})][1 + \pi\gamma^2 g(\Delta_{f_1})]} \\ & \left. + \frac{g(\Delta_{i_1})g(\Delta_{f_0})}{(\Delta_{i_1} - \Delta_{f_1})[1 + \pi\gamma^2 g(\Delta_{i_1})][1 + \pi\gamma^2 g(\Delta_{f_0})]} \right]. \end{aligned} \quad (\text{E6})$$

We can rearrange the frequency-conserving terms and again substitute the definition of $g(\Delta)$ into the frequency-mixing term to determine

$$\begin{aligned} \mathcal{A} = & t(i_0)t(i_1)[\delta(f_0 - i_0)\delta(f_1 - i_1) + \delta(f_0 - i_1)\delta(f_1 - i_0)] \\ & + \frac{2\pi i\gamma^4 \delta(f_0 + f_1 - i_0 - i_1)}{[\Delta_{f_0} + i\pi\gamma^2][\Delta_{f_1} + i\pi\gamma^2]} \left[\frac{\Delta_{f_1} + i\pi\gamma^2}{(\Delta_{f_1} - \Delta_{i_0})[\Delta_{i_0} + i\pi\gamma^2]} + \frac{\Delta_{f_0} + i\pi\gamma^2}{(\Delta_{f_0} - \Delta_{i_0})[\Delta_{i_0} + i\pi\gamma^2]} \right. \\ & \left. + \frac{\Delta_{f_0} + i\pi\gamma^2}{(\Delta_{f_0} - \Delta_{i_1})[\Delta_{i_1} + i\pi\gamma^2]} + \frac{\Delta_{f_1} + i\pi\gamma^2}{(\Delta_{f_1} - \Delta_{i_1})[\Delta_{i_1} + i\pi\gamma^2]} \right]. \end{aligned} \quad (\text{E7})$$

Straight-forward algebraic manipulation of Eq. (E7) then leads us to

$$\begin{aligned} \mathcal{A} = & t(i_0)t(i_1)[\delta(f_0 - i_0)\delta(f_1 - i_1) + \delta(f_0 - i_1)\delta(f_1 - i_0)] \\ & + \frac{4\pi i\gamma^4 \delta(f_0 + f_1 - i_0 - i_1)}{[\Delta_{f_0} + i\pi\gamma^2][\Delta_{f_1} + i\pi\gamma^2]} \\ & \left(\frac{1}{\Delta_{i_0} + i\pi\gamma^2} + \frac{1}{\Delta_{i_1} + i\pi\gamma^2} \right) \end{aligned} \quad (\text{E8})$$

which is the result by Fan *et al.*

Appendix F: Single Photon State Vector Evolution

In this appendix we include explicit details of the single photon entanglement generation calculation. The state

input to the Mach-Zehnder interferometer is given by

$$|\Psi_{\text{in}}\rangle = \frac{1}{2} [|i\rangle (|u\rangle + |g\rangle) |0\rangle (|u\rangle + |g\rangle)], \quad (\text{F1})$$

where successive kets label the optical and emitter states in the upper and lower interferometer arms respectively. Applying the beam-splitter transformation, it is possible to determine that

$$|\Phi_{\text{in}}\rangle = \frac{1}{2\sqrt{2}} [|i\rangle (|u\rangle + |g\rangle) |0\rangle (|u\rangle + |g\rangle) - |0\rangle (|u\rangle + |g\rangle) |i\rangle (|u\rangle + |g\rangle)]. \quad (\text{F2})$$

States with a photon and $|g\rangle$ atomic component then acquire a phase-shift \mathcal{A} —as calculated in the main text—and we have

$$|\Phi_{\text{out}}\rangle = \frac{1}{2\sqrt{2}} [|i\rangle (|u\rangle + \mathcal{A}|g\rangle) |0\rangle (|u\rangle + |g\rangle) - |0\rangle (|u\rangle + |g\rangle) |i\rangle (|u\rangle + \mathcal{A}|g\rangle)]. \quad (\text{F3})$$

After applying the second beam-splitter transformation and some algebra, we find

$$|\Psi_{\text{out}}\rangle = \frac{1}{4} [|i\rangle (|u\rangle + \mathcal{A}|g\rangle) |0\rangle (|u\rangle + |g\rangle) - |0\rangle (|u\rangle + \mathcal{A}|g\rangle) |i\rangle (|u\rangle + |g\rangle) - |0\rangle (|u\rangle + \mathcal{A}|g\rangle) |i\rangle (|u\rangle + |g\rangle) - |i\rangle (|u\rangle + \mathcal{A}|g\rangle) |0\rangle (|u\rangle + |g\rangle)]. \quad (\text{F4})$$

From this we can determine the probabilities of detecting photons in each interferometer arm and the subsequent reduced atomic density matrices.

-
- [1] R. Raussendorf and H. J. Briegel, *Phys. Rev. Lett.* **86**, 5188 (2001).
- [2] H. J. Kimble, *Nature* **453**, 1023 (2008).
- [3] A. Reiserer and G. Rempe, *Rev. Mod. Phys.* **87**, 1379 (2015).
- [4] P. Facchi, M. S. Kim, S. Pascazio, F. V. Pepe, D. Pomarico, and T. Tufarelli, *Phys. Rev. A* **94**, 043839 (2016).
- [5] P. Facchi, S. Pascazio, F. V. Pepe, and K. Yuasa, ArXiv e-prints (2017), [arXiv:1705.01967](https://arxiv.org/abs/1705.01967) [quant-ph].
- [6] A. Sipahigil, R. E. Evans, D. D. Sukachev, M. J. Burek, J. Borregaard, M. K. Bhaskar, C. T. Nguyen, J. L. Pacheco, H. A. Atikian, C. Meuwly, R. M. Camacho, F. Jelezko, E. Bielejec, H. Park, M. Lončar, and M. D. Lukin, *Science* (2016), [10.1126/science.aah6875](https://doi.org/10.1126/science.aah6875).
- [7] P. Lodahl, S. Mahmoodian, S. Stobbe, A. Rauschenbeutel, P. Schneeweiss, J. Volz, H. Pichler, and P. Zoller, *Nature* **541**, 473 (2017).
- [8] I. Söllner, S. Mahmoodian, S. L. Hansen, L. Midolo, A. Javadi, G. Kiršanskė, T. Pregmolato, H. El-Ella, E. H. Lee, J. D. Song, S. Stobbe, and P. Lodahl, *Nat Nano* **10**, 775 (2015).
- [9] R. Coles, D. Price, J. Dixon, B. Royall, E. Clarke, P. Kok, M. Skolnick, A. Fox, and M. Makhonin, *Nature Communications* **7**, 11183 EP (2016).
- [10] S. Fan, S.E. Kocabas, and J. T. Shen, *Phys. Rev. A* **82**, 063821 (2010).
- [11] S. Xu and S. Fan, *Phys. Rev. A* **91**, 043845 (2015).
- [12] T. Caneva, M. Manzoni, T. Shi, J. Douglas, J. I. Cirac, and D. E. Chang, *New Journal of Physics* **17**, 113001 (2015).
- [13] T. Shi, D. E. Chang, and J. I. Cirac, *Phys. Rev. A* **92**, 053834 (2015).
- [14] T. Shi and C. P. Sun, *Phys. Rev. B* **79**, 205111 (2009).
- [15] S. Xu, E. Rephaeli, and S. Fan, *Phys. Rev. Lett.* **111**, 223602 (2013).
- [16] T. F. See, C. Noh, and D. G. Angelakis, *Phys. Rev. A* **95**, 053845 (2017).
- [17] W. Konyk and J. Gea-Banacloche, *Phys. Rev. A* **93**, 063807 (2016).
- [18] T. Shi, Y. Chang, and J. J. Garcia-Ripoll, ArXiv e-prints (2017), [arXiv:1701.04709](https://arxiv.org/abs/1701.04709) [quant-ph].
- [19] A. Nysteen, P. T. Kristensen, D. P. S. McCutcheon, P. Kaer, and J. Mørk, *New Journal of Physics* **17**, 023030 (2015).
- [20] S. D. Barrett and P. Kok, *Phys. Rev. A* **71**, 060310 (2005).
- [21] G. Z. Cohen and L. J. Sham, *Phys. Rev. B* **88**, 245306 (2013).
- [22] A. Javadi, I. Söllner, M. Arcari, S. L. Hansen, L. Midolo, S. Mahmoodian, G. Kiršanskė, T. Pregmolato, E. H. Lee, J. D. Song, S. Stobbe, and P. Lodahl, *Nature Communications* **6**, 8655 EP (2015).
- [23] M. Schwartz, *Quantum Field Theory and the Standard Model* (Cambridge University Press, 2014).
- [24] N. Quesada and J. E. Sipe, *Phys. Rev. A* **90**, 063840 (2014).
- [25] A. Brańczyk, *Non-classical States of Light*, Ph.D. thesis, University of Queensland (2010).
- [26] M. Spivak, *Calculus*, Addison-Wesley world student series (Publish or Perish, 1980).
- [27] W. K. Wootters, *Phys. Rev. Lett.* **80**, 2245 (1998).
- [28] C. K. Hong, Z. Y. Ou, and L. Mandel, *Phys. Rev. Lett.* **59**, 2044 (1987).
- [29] S. Maier, “Plasmonics: Fundamentals and applications,” (Springer US, Boston, MA, 2007) Chap. Surface Plasmon Polaritons at Metal / Insulator Interfaces, pp. 21–37.
- [30] G. Arfken and H. Weber, *Mathematical Methods For Physicists International Student Edition* (Elsevier Science, 2005).